

引用格式：李宗耀，盛美，蒋凯，等，2022. 青藏高原东北缘西宁黄土物源研究 [J]. 地质力学学报, 28 (4): 605–616. DOI: 10.12090/j.issn.1006-6616.2022029

Citation: LI Z Y, SHENG M, JIANG K, et al., 2022. Provenance study of the Xining loess in the Northeastern Tibetan Plateau [J]. Journal of Geomechanics, 28 (4): 605–616. DOI: 10.12090/j.issn.1006-6616.2022029

青藏高原东北缘西宁黄土物源研究

李宗耀^{1,2}, 盛 美^{1,2,3}, 蒋 凯¹, 易施钰^{1,2}, 王喜生^{1,2}

LI Zongyao^{1,2}, SHENG Mei^{1,2,3}, JIANG Kai¹, YI Shiyu^{1,2}, WANG Xisheng^{1,2}

1. 中国地质科学院地质力学研究所, 北京 100081;
2. 自然资源部古地磁与古构造重建重点实验室, 北京 100081;
3. 中国地质调查局极地地学研究中心, 北京 100081

1. Institute of Geomechanics, Chinese Academy of Geological Sciences, Beijing 100081, China;
2. Key Laboratory of Paleomagnetism and Tectonic Reconstruction, Ministry of Natural Resources, Beijing 100081, China;
3. Research Center of Polar Geosciences, China Geological Survey, Beijing 100081, China

Provenance study of the Xining loess in the Northeastern Tibetan Plateau, China

Abstract: Single-grain U-Pb dating of detrital zircons is regarded as an efficient and effective technique to differentiate the contribution of discrete sources. However, its application to the extensive Chinese Loess Plateau (CLP) yields rather complex information in provenance discrimination. The Xining loess was deposited in the Northeastern Tibetan Plateau (NETP), and the detrital zircon U-Pb chronology study can not only obtain provenance information but also provide an important basis to discuss the contribution of the detrital materials from the Northern Tibetan Plateau (NTP) to the CLP. Results of the detrital zircon morphology suggest that zircons may have undergone intense physical weathering and multiple recirculations, and may also indicate the high complexity of the source. Detrital zircon U-Pb age results from different sedimentary layers of the Xining loess reveal there are no obvious temporal variations in the provenance of the Xining loess since ~1.3 Ma and materials may ultimately be eroded from the NTP and the Central Asian Orogenic Belt (CAOB), although the relative contribution of detritus from the two sources may slightly vary through time. The U-Pb age spectra of the Xining loess are highly similar to that of typical loess sites in the western-central CLP, suggesting that the provenance areas of the CLP and the Xining loess may be largely consistent, but the possibility of a small difference of provenance cannot be ruled out.

Keywords: Xining; detrital zircon; U-Pb ages; provenance; Chinese Loess Plateau; Northeastern Tibetan Plateau

摘要：碎屑锆石 U-Pb 年代学被认为是研究沉积物物源的有效手段。然而，应用碎屑锆石 U-Pb 年代学对中国黄土高原进行物源研究时却获得了非常复杂的物源信息。西宁黄土沉积于青藏高原东北缘地区，对其开展碎屑锆石 U-Pb 年代学研究不仅可以获得其物源信息，同时可以为探讨青藏高原北缘碎屑物质对黄土高原的贡献提供重要依据。碎屑锆石形貌学研究结果表明其可能经历了强烈的物理风化以及多次再循环，同时也可能暗示了物源的高度复杂性。来自不同沉积层位的碎屑锆石 U-Pb 年龄结果表明，西宁黄土碎屑物质的最终来源可能是青藏高原北缘和中亚造山带，且物源区自约 1.3 Ma 以来可能没有显著变化，但是两者对西宁黄土的相对贡献可能在不同的时期具有微弱的差异。西宁黄土与中国黄土高原中、西部典型剖面的碎屑锆石年龄分布具有高度相似性，暗示了两者的物源区可能很大程度上具有一致性，但具少量差异。

基金项目：国家自然科学基金（42074078, 41672178, 42104080）

This research is financially supported by the National Natural Science Foundation of China (Grants No. 42074078, 41672178, 42104080)

第一作者简介：李宗耀（1993—），男，在读博士，主要从事黄土环境磁学研究。E-mail: lyyslzy@126.com

收稿日期：2022-03-08；修回日期：2022-07-15；责任编辑：吴芳

关键词：西宁；碎屑锆石；U-Pb 年龄；物源；中国黄土高原；青藏高原东北缘

中图分类号：P611, P618 文献标识码：A 文章编号：1006-6616 (2022) 04-0605-12

DOI: 10.12090/j.issn.1006-6616.2021143

0 引言

中国黄土高原的风尘堆积记录了第四纪时期最高分辨率的全球气候变化 (Liu and Ding, 1998; An, 2000; Maher, et al., 2010)。刘东生 (1985) 发现中国黄土高原的黄土堆积自西北部至东南部，厚度逐渐变薄，粒度逐渐变细，暗示了风尘可能主要来源于黄土高原西北部广大的戈壁、沙漠地区。来自地球化学、矿物学方面的证据表明蒙古戈壁-沙漠南部和阿拉善干旱区是亚洲风尘主要物源地，其碎屑物质最终来源于中亚造山带的戈壁阿尔泰山脉和青藏高原北缘 (Ji, et al., 1999; Chen, et al., 2007; Li, et al., 2007; Sun, et al., 2008; Li, et al., 2009; Chen and Li, 2011)。

碎屑锆石 U-Pb 年代学分析为沉积物物源的研究做出了巨大的贡献 (郭佩等, 2017; 程瑜等, 2018; 林旭等, 2021)。然而，该技术在黄土物源的研究中提供了有力地证据，同时也带来了更加复杂的物源信息。黄土高原西北部北郭塬黄土的碎屑锆石年代学研究表明其与近源的沙漠没有单一的亲缘关系，主要来自于祁连山脉和塔克拉玛干沙漠 (Stevens et al., 2010)。Pullen et al. (2011) 发现洛川黄土与柴达木盆地第四纪沉积物具有一致的碎屑锆石年龄分布特征，表明青藏高原北缘，尤其是柴达木盆地，对黄土高原的碎屑物质具有重要的贡献。随后的一些研究进一步支持了包括柴达木盆地的青藏高原北缘是黄土高原重要的物源区的观点 (Che and Li, 2013; Bird et al., 2015; Licht et al., 2016; Zhang et al., 2016, 2018; Fenn et al., 2018)。近年来，一些研究基于黄土高原、西毛乌素沙地、黄河沉积物与青藏高原东北缘具有相似的碎屑锆石年龄分布，认为青藏高原东北缘剥蚀下来的碎屑物质通过黄河的搬运被输送至毛乌素沙地和黄土高原 (Stevens et al., 2013a; Nie et al., 2015; Zhang et al., 2021)。基于塔里木盆地、准噶尔盆地、柴达木盆地沉积物和黄土高原北部靖边黄土的碎屑锆石年龄分析，Sun et al. (2018) 提出黄土的物源区主要是中亚

造山带、祁连山脉和华北克拉通，而不是塔里木盆地、准噶尔盆地和柴达木盆地。Sun et al. (2020) 对黄土源-汇系统综合分析提出亚洲风尘具有 3 个主要物源 (青藏高原北缘、中亚造山带和鄂尔多斯高原) 及 10 个次要物源 (古尔班通右特沙漠、蒙古戈壁沙漠、塔克拉玛干沙漠、巴丹吉林沙漠、腾格里沙漠、柴达木盆地、库布奇沙漠、毛乌素沙地、浑善达克沙地和科尔沁沙地)。

除了主要物源区对黄土沉积的相对贡献具有争论外，黄土高原的物源是否具有空间一致性也具有争议 (Jahn et al., 2001; Maher et al., 2009; Xiao et al., 2012; Che and Li., 2013; Bird et al., 2015; Zhang et al., 2021)。来自于黄土高原不同黄土剖面的碎屑锆石年代学研究提出了黄土高原不同地区的黄土可能来自不同的物源区，这明显不同于基于地球化学、同位素等证据提出的黄土高原物源区具有空间一致性的观点 (Jahn et al., 2001; Maher et al., 2009)。此外，黄土高原物源的时间变化同样是一个具有争议的问题。Xiao et al. (2012) 基于碎屑锆石 U-Pb 年代学研究认为黄土-古土壤层位的物源具有差异，而 Che and Li (2013) 基于同样的研究方法不认为存在黄土-古土壤层位物源差异。Stevens et al. (2013b) 和 Fenn et al. (2017) 利用地球化学与矿物学研究发现在北郭塬~20 ka 时期物源发生突变。另外，黄土-古土壤层位锆石 U-Pb 年龄和重矿物组分的统计研究表明这些矿物的物源并未发生变化 (Nie et al., 2014; Licht et al., 2016)。因此，黄土-古土壤序列物源是否具有时间差异需要更多证据的支持。

西宁盆地位于黄土高原东邻，保存有青藏高原东北缘地区最大、最厚的黄土堆积。矿物学研究认为青藏高原东北缘的黄土堆积主要来自于青藏高原内部 (李珍和聂树人, 1999)。然而，碎屑锆石年代学研究发现末次冰期的西宁黄土与黄土高原内部黄土具有可对比性 (李高军等, 2013)。西宁黄土位于青藏高原东北缘的碎屑物质向东输送至黄土高原的重要路径上，对西宁黄土的碎屑锆石年代学研究，不仅能反映其本身的物源信息，同时对黄土高原的物源研究具有重要意义。基于

此, 选择西宁黄土 1.3 Ma 以来不同黄土层位进行碎屑锆石形貌学及 U-Pb 年龄分析, 通过对比, 研究西宁黄土主要物源区及其可能存在的时间变化, 以及探讨青藏高原东北缘黄土与黄土高原内部黄土物源的空间差异。

1 样品采集与实验方法

1.1 研究区概况及样品采集

研究区位于青藏高原东北缘西宁盆地内,

盆地北、西、南侧被祁连山及其支脉——拉脊山、日月山包围, 东侧与黄土高原相邻(图 1)。在自然地理区域上, 西宁盆地位于西北内陆干旱区、东部季风区与高原季风影响的边界地带。盆地平均海拔约 2000 m, 全年平均气温约 6 ℃, 平均降水量约 400 mm(中国气象数据网)。湟水自西向东穿过西宁盆地中心, 切穿盆地内新生代地层。第四纪黄土沉积于湟水阶地之上, 尤以西宁城北大墩岭沉积的黄土地层最厚、最具代表性。

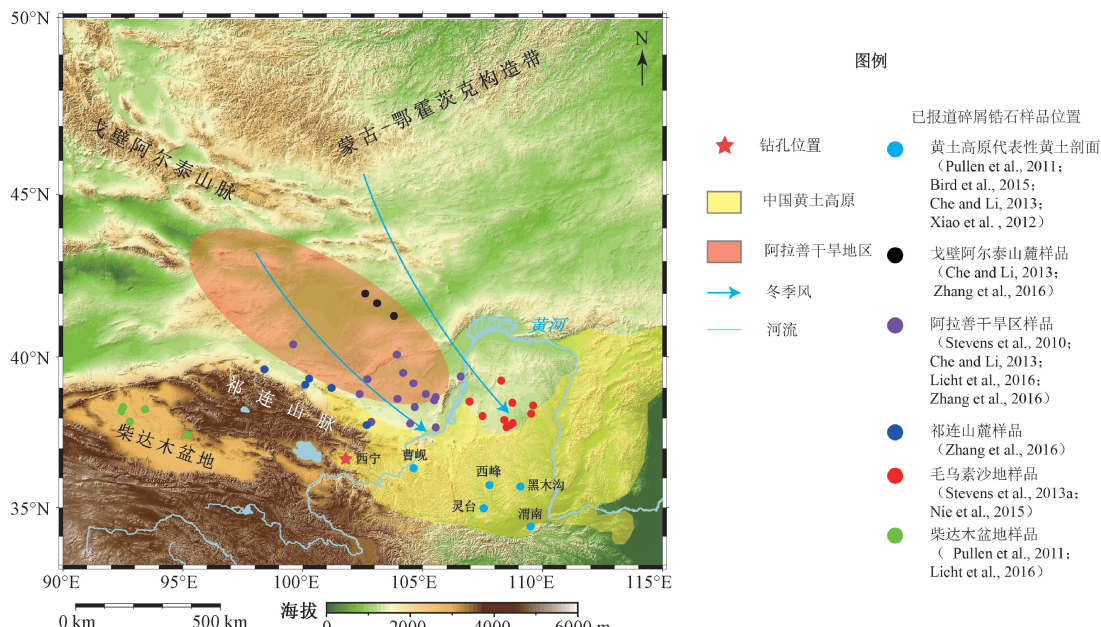


图 1 研究区自然地理背景及碎屑锆石样品位置

Fig. 1 Geographical setting of the research area and detrital zircon sample sites

在大墩岭顶部稳定塬面(36.65°N ; 101.79°E)进行科学钻探, 钻井海拔为 2740 m, 深度为 261 m。钻探获得 260.4 m 厚的黄土-古土壤沉积序列以及底部的冲积砾石层岩芯。将岩芯从中间剖开, 以 10 cm 间距采样进行磁化率测试。结合 Lu et al. (2012) 的岩性和古地磁学研究, 以及此次的磁化率研究结果, 对岩芯进行地层学划分, 结果表明大墩岭黄土-古土壤序列底部为 S_{16} , 年龄为约 1.3 Ma(图 2)。在 S_2LL_1 (2.2~4.6 m)、 L_5 (56~57.5 m)、 L_7 (118~120 m)、 L_9 (150~152.5 m) 和 L_{13} (210~212.5 m) 等层位采集 5 个混合样品, 命名为 DL-1、DL-2、DL-3、DL-4 和 DL-5, 进行碎屑锆石 U-Pb 年代学分析。

1.2 测试方法

每个样品均取约 5 kg 黄土, 采用常规浮选与

磁选法进行矿物分选, 得到数百颗锆石颗粒, 再在显微镜下挑选出 200 颗左右锆石颗粒制靶, 拍摄锆石反射光、透射光和阴极发光(CL)显微照片。选择锆石无裂隙区域作为靶区, 使用 Agilent7900 MS 等离子体质谱仪与 ESI NWR 193 nm 激光剥蚀系统进行锆石 U-Pb 测年。使用 NIST 610 作为校正 U、Th 和 Pb 含量的标准样品, GJ-1 作为校正仪器偏差的标准样品, 91500 作为校正同位素分馏的标准样品。每个样品测试了 120 颗碎屑锆石, 去掉谐和度<90% 的锆石, 5 个样品分别获得了 111、117、112、107 和 108 个有效年龄。对于 $^{206}\text{Pb}/^{238}\text{U}$ 年龄 <1000 Ma 的锆石颗粒, 采用 $^{206}\text{Pb}/^{238}\text{U}$ 年龄, 对于 $^{206}\text{Pb}/^{238}\text{U}$ 年龄 > 1000 Ma 的锆石颗粒, 采用 $^{207}\text{Pb}/^{206}\text{Pb}$ 年龄。使用 DensityPlotter 程序 (Vermeesch, 2012) 绘制锆石 U-Pb 年龄的直方图与核密度估计(KDE)图。

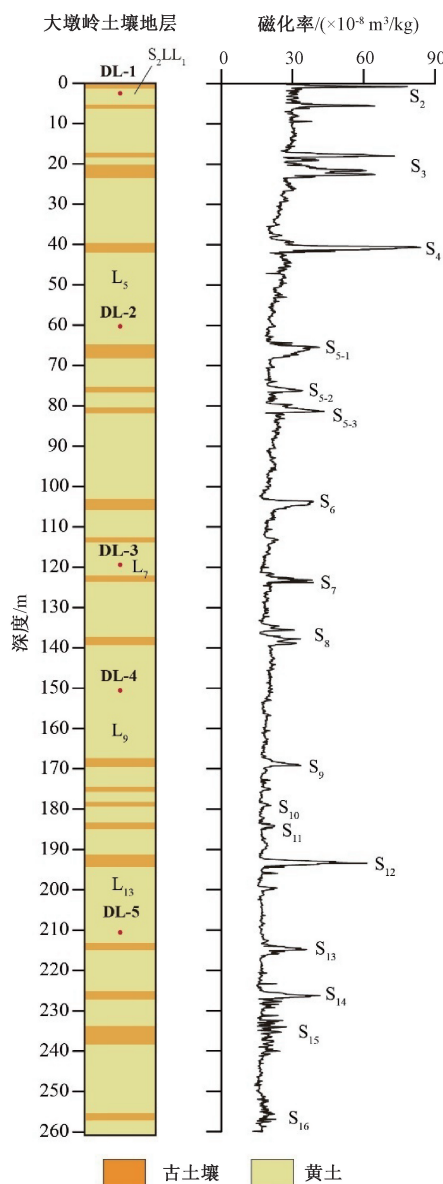


图 2 大墩岭钻探岩芯的土壤地层和磁化率随深度变化

Fig. 2 Pedostratigraphy and magnetic susceptibility variations with depth in the Dadunling core

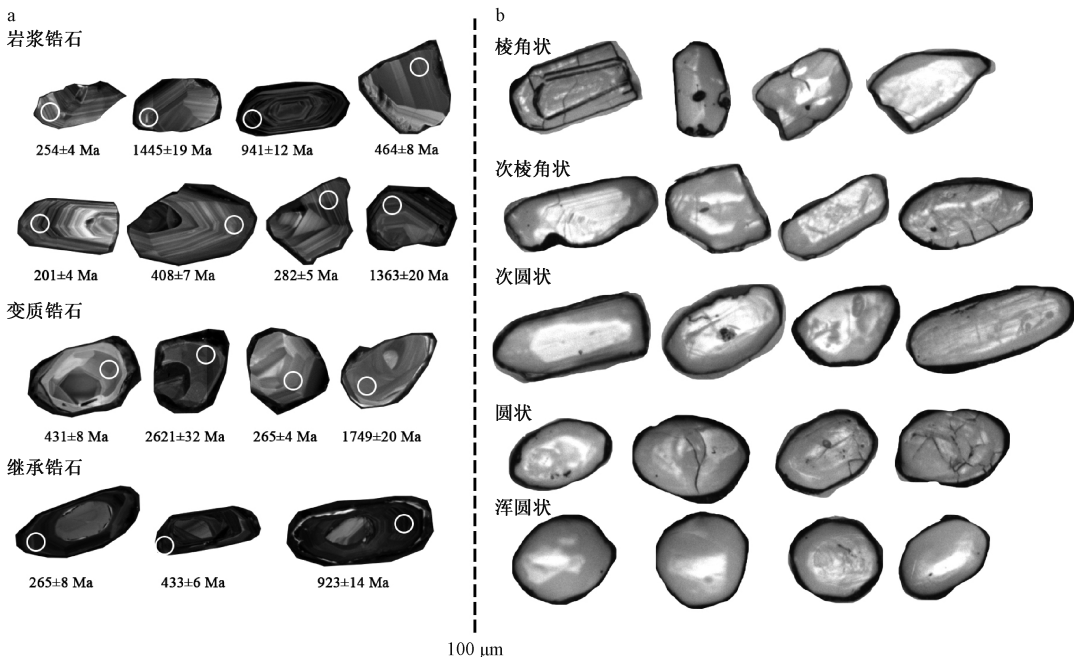
1.3 锆石形貌学

锆石阴极发光照片可以观察锆石的结构和环带特征。分析的锆石粒径为约 $40 \sim 200 \mu\text{m}$ ，通过锆石 CL 图反映的内部结构，可将锆石分为岩浆锆石、变质锆石和继承锆石（图 3a）。反射光图可清晰地反映锆石表面的磨圆情况，绝大多数锆石具有不同程度的磨圆。根据锆石表明磨圆程度不同，将锆石分为棱角状、次棱角状、次圆状、圆状和浑圆状 5 类（图 3b），对反射光图中所有的碎屑锆石进行磨圆度统计，结果见表 1。西宁黄土中锆石棱角状占比 $5.9\% \sim 13.9\%$ ，次棱角状占比

$27.5\% \sim 48.7\%$ ，次圆状占比 $24.5\% \sim 37.6\%$ ，圆状占比 $8.8\% \sim 22.0\%$ ，浑圆状占比 $1.5\% \sim 5.9\%$ 。整体来看，棱角状与次棱角状的碎屑锆石占全部样品总数的 49.0% ，可能暗示了西宁黄土存在一个距离较近的物源区。西宁黄土碎屑锆石具有多种类型的混合、复杂的磨圆度与裂隙的发育等特征，表明锆石颗粒可能经历了强烈的物理风化以及多次再循环，同时也可能暗示了多物源的混合。

2 结果与讨论

从不同层位采集的 5 个样品具有基本一致的锆石 U-Pb 年龄分布，可划分为 4 个年龄组：早中生代—古生代 ($200 \sim 540 \text{ Ma}$)，新元古代 ($540 \sim 1000 \text{ Ma}$)，中元古代早期—古元古代中期 ($1400 \sim 2050 \text{ Ma}$) 和古元古代早期—新太古代 ($2300 \sim 2800 \text{ Ma}$)（图 4）。5 个样品共 555 个锆石，年龄只有 3 个 $<200 \text{ Ma}$: $197 \pm 4 \text{ Ma}$ (DL-1)， $190 \pm 3 \text{ Ma}$ (DL-4) 和 $195 \pm 4 \text{ Ma}$ (DL-4)。显生宙年龄组在西宁黄土中占大多数，占比约 $42\% \sim 58\%$ ，且具有显著的双峰特征，峰值年龄分别为约 250 Ma 和约 420 Ma ，其余 3 个年龄组占比分别为 $11\% \sim 22\%$ ($540 \sim 1000 \text{ Ma}$)、 $13\% \sim 19\%$ ($1400 \sim 2050 \text{ Ma}$) 和 $8\% \sim 12\%$ ($2300 \sim 2800 \text{ Ma}$)。西宁黄土除具约 250 Ma 和约 420 Ma 主要年龄峰值外，还具有 800 Ma 、 1800 Ma 和 2500 Ma 次要年龄峰值。5 个样品不同年龄组的相对含量具有轻微的差异。与其他峰值年龄相比，约 250 Ma 峰值年龄的锆石相对含量具有更明显的变化。此外，样品 DL-1 中元古代早期 (约 1500 Ma) 锆石含量明显较其他层位少。这种在基本一致的锆石年龄分布下，不同年龄组相对含量的轻微差异，可能反映了不同物源在不同时期对西宁黄土的贡献具有轻微的变化。西宁黄土与黄土高原中—西部已报道黄土剖面的锆石年龄谱高度相似（图 5），年龄分布基本一致，均具有约 250 Ma 、约 420 Ma 、约 800 Ma 、约 1850 Ma 和约 2450 Ma 的峰值年龄。但是，在 $<190 \text{ Ma}$ 组分含量上，西宁黄土和黄土高原黄土具有差异。在黄土高原腹地的黑木沟、灵台、西峰和渭南黄土剖面中含有少量该年龄组分锆石（图 5a—5d），在黄土高原西部的曹岘黄土剖面，该年龄组分锆石相比黄土高原腹地的黄土剖面含量显著减少（图 5e），而在更往西的西宁黄土，则未发现该年龄组



a—阴极发光 (CL) 图; b—反射光图

图3 西宁黄土代表性碎屑锆石显微照片

Fig. 3 Micrographs of representative detrital zircons from the Xining loess

(a) Cathode luminescence (CL) images; (b) Reflected light images

表1 西宁黄土碎屑锆石磨圆度统计结果

Table 1 Statistical results of detrital zircon roundness of the Xining loess

	棱角状	次棱角状	次圆状	圆状	浑圆状	总数目
DL-1	7.9%	45.3%	31.8%	11.2%	3.7%	267
DL-2	9.0%	27.5%	37.6%	22.0%	3.9%	255
DL-3	5.9%	38.1%	35.9%	14.3%	5.9%	273
DL-4	13.9%	48.7%	24.5%	8.8%	3.3%	271
DL-5	11.4%	38.5%	35.2%	13.6%	1.5%	273

分锆石(图5f)。这种碎屑锆石年龄分布基本一致,但是在<190 Ma组分含量存在差异的情况,可能暗示了西宁黄土和黄土高原黄土的物源区在基本一致的情况下,存在一处物源区为黄土高原提供了少量碎屑物质,造成<190 Ma锆石含量差异。

200~300 Ma和400~500 Ma分别是海西—印支期造山运动和加里东期造山运动活跃的时期。西宁黄土与中国黄土高原的锆石年龄以200~300 Ma和400~500 Ma为主(图6a、6b),暗示了物源区在这两个时期具有大规模的构造运动。大量的研究表明,祁连山脉、柴达木盆地、库木塔格沙漠、阿拉善干旱区和毛乌素沙漠碎屑锆石年龄以约200~500 Ma为主,其中阿拉善干旱区、西毛乌素沙地以约200~300 Ma峰值为主,祁连山脉和柴达木盆地以约400~500 Ma为主(图6c—6h); Stevens, et al., 2010; Pullen et al., 2011; Che and

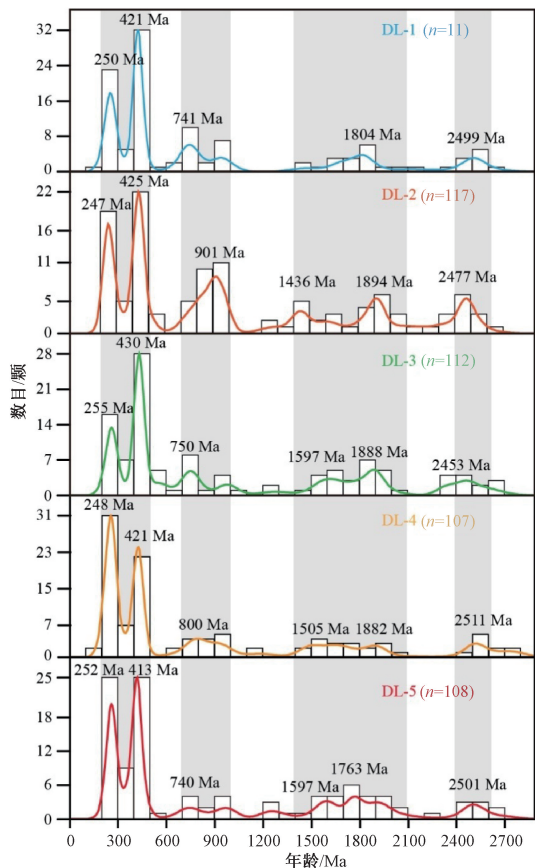
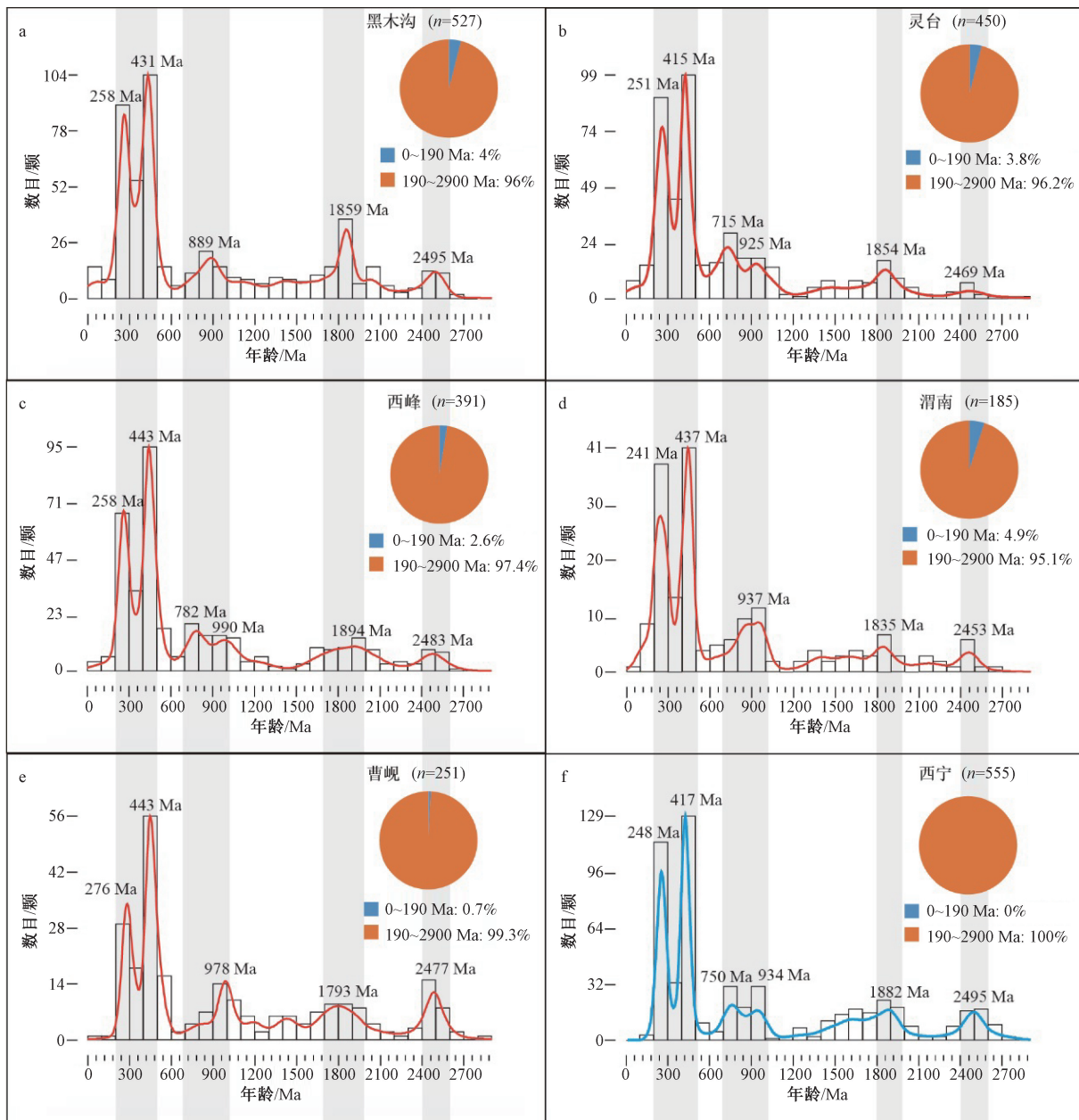
图4 西宁黄土碎屑锆石U-Pb年龄结果(n 为锆石数目)

Fig. 4 Detrital zircon U-Pb age histograms of the Xining loess



a—黑木沟剖面 (Pullen et al., 2011); b—灵台剖面 (Bird et al., 2015); c—西峰剖面 (Che and Li, 2013); d—渭南剖面 (Xiao et al., 2012); e—曹岘剖面 (Che and Li, 2013); f—西宁黄土

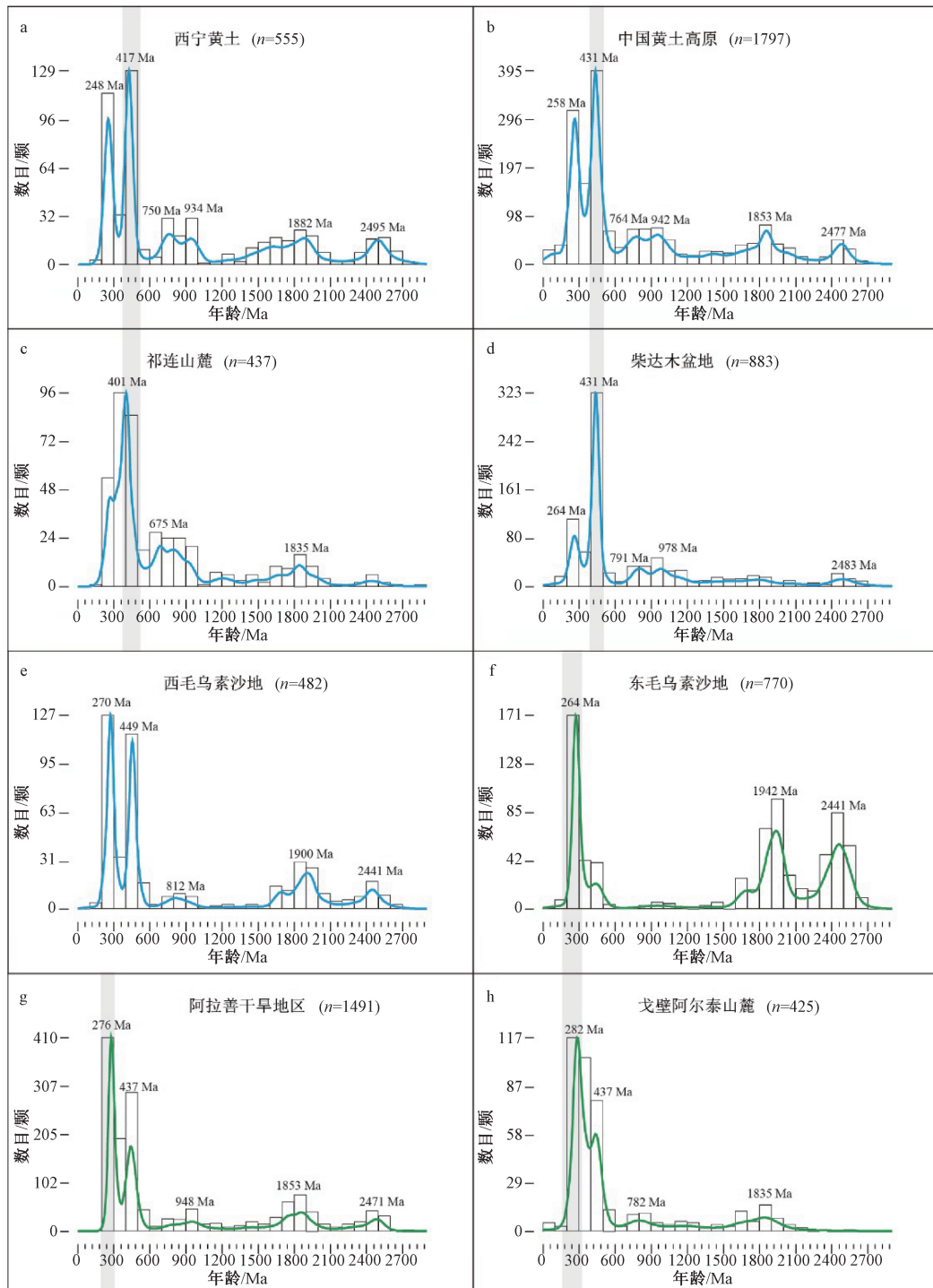
图 5 碎屑锆石 U-Pb 年龄直方图及 KDE 图 (n 为锆石数目)

Fig. 5 Detrital zircon U-Pb age histograms and KDE diagrams

(a) The Heimugou section (Pullen et al., 2011); (b) The Lingtai section (Bird et al., 2015); (c) The Xifeng section (Che and Li, 2013); (d) The Weinan section (Xiao et al., 2012); (e) The Caoxian section (Che and Li, 2013); (f) The Xining loess

Li, 2013; Licht et al., 2016; Zhang et al., 2016)。西宁盆地位于毛乌素沙地的西南方，并不处于毛乌素沙地碎屑物质随冬季风搬运的沉积区，因此毛乌素沙地不太可能是西宁黄土的主要物源。阿拉善干旱区沉积物的 Sr-Nd 同位素研究表明其是来自于青藏高原北缘和中亚造山带碎屑物质的混合 (Li et al., 2011)。青藏高原北缘作为黄土的潜在

物源区，其碎屑物质可能来源于柴达木盆地、祁连山脉以及阿尔金山脉。对于祁连山脉与阿尔金山脉，在早古生代时期的俯冲、碰撞事件中可能发生了大规模的岩浆、变质活动 (Wu et al., 2009, 2018; Song et al., 2013, 2014; Yang et al., 2015; 夏林圻等, 2016, Yu et al., 2018)。祁连山脉内河流沉积物的碎屑锆石年龄谱具有显著的约



a—西宁黄土样品; b—黑木沟、西峰、灵台、渭南、曹岘 5 个黄土剖面综合数据; c—祁连山麓沉积物 (Zhang et al., 2016); d—柴达木盆地沉积物 (Pullen et al., 2011; Licht et al., 2016); e—西毛乌素沙地沉积物 (Stevens et al., 2013a; Nie et al., 2015); f—东毛乌素沙地沉积物 (Stevens et al., 2010, 2013; Nie et al., 2015); g—阿拉善干旱区 (综合的腾格里沙漠、弱水河床沉积物样品数据, 引自 Stevens et al., 2010; Che and Li, 2013; Licht et al., 2016; Zhang et al., 2016); h—戈壁阿尔泰山麓沉积物 (Che and Li, 2013; Zhang et al., 2016)

图 6 西宁黄土、黄土高原及潜在物源区沉积物的碎屑锆石 U-Pb 年龄直方图与 KDE 图 (n 为锆石数目)

Fig. 6 Detrital zircon U-Pb chronology of the Xining loess, the CLP and potential provenances and KDE diagrams

(a) Samples from the Xining loess; (b) Combined data of the five loess sections of the CLP in Figure 4; (c) Sediments from the piedmont of the Qilian mountains (Zhang et al., 2016); (d) Sediments from the Qaidam Basin (Pullen et al., 2011; Licht et al., 2016); (e) Sediments from the western Mu Us desert (Stevens et al., 2013a; Nie et al., 2015); (f) Sediments from the eastern Mu Us desert (Stevens et al., 2010, 2013; Nie et al., 2015); (g) Alxa arid areas (Combined data from the Tengger Desert and the Ruoshui River, after Stevens et al., 2010; Che and Li, 2013; Licht et al., 2016; Zhang et al., 2016); (h) Sediments from the piedmont of the Gobi Altay mountains (Che and Li, 2013; Zhang et al., 2016)

439 Ma 年龄峰值，并指示沉积物中含有少量的 200~300 Ma 锆石 (Zhang et al., 2020)。柴达木盆地沉积物碎屑锆石年龄谱的约 431 Ma 主要峰值和约 264 Ma 次要峰值，表明其含有的约 380~490 Ma 锆石主要来自于祁连山脉与阿尔金山脉 (Pullen et al., 2011; Licht et al., 2016)。

中亚造山带作为地球上最大的显生宙增生造山带 (Windley et al., 2007)，含有 3 个二叠纪—三叠纪拼贴系统 (Zhang et al., 2009; Xiao et al., 2009, 2015)。中亚造山带二叠纪—三叠纪时期广泛发育的岩浆活动 (Miao et al., 2007; Jian et al., 2008; Chu et al., 2013; Zheng et al., 2014; 贺昕宇等, 2022) 可以为附近的沙漠提供约 200~300 Ma 锆石。中亚造山带的戈壁-阿尔泰山脉被认为是黄土高原主要的物源区 (Chen et al., 2007; Li et al., 2009, 李高军等, 2013; Che and Li, 2013; Zhang et al., 2016, 2018)，其山麓沉积物的碎屑锆石年龄以 250~400 Ma 为主 (图 6h; Che and Li, 2013; Zhang et al., 2016)。相较于大规模的晚古生代岩浆活动，中亚造山带早古生代岩浆活动则分布有限。在中国西北部，中亚造山带的早古生代的岩浆活动主要分布于北山造山带和天山山脉 (徐学义等, 2008; Li et al., 2016; Yuan et al., 2018)。天山山脉早古生代岩浆活动主要发育于 300~400 Ma (Li et al., 2016)，山脉北麓准噶尔盆地新生代沉积物碎屑锆石年代学研究表明主要年龄组分为 300~350 Ma (陈熠等, 2012)。结合 Sr-Nd 同位素研究结果及黄土潜在物源区沉积物、其他黄土剖面的碎屑锆石年代学研究结果 (Gehrels et al., 2003; 谢静等, 2007; Stevens et al., 2010; Xie et al., 2012; Xiao et al., 2012; Che and Li, 2013; Licht et al., 2016)，西宁黄土主要的年龄组分约 200~500 Ma 的碎屑锆石可能主要来自中亚造山带和青藏高原北缘。鉴于近青藏高原北缘地区沉积物中含有大量早古生代碎屑锆石，近中亚造山带地区沉积物中含有大量晚古生代碎屑锆石 (图 6)，因此西宁黄土中 200~300 Ma 年龄组分的碎屑锆石可能主要由中亚造山带提供，而 400~500 Ma 年龄组分的碎屑锆石则主要由青藏高原北缘提供。

西宁黄土 L₉ 样品中的约 250 Ma 峰值年龄的锆石含量较约 420 Ma 峰值年龄的锆石含量高，而其他样品则是约 250 Ma 峰值年龄的锆石含量较少。

由于 L₉ 是 1.1 Ma 以来厚度最大、粒度最粗的黄土层位，代表了一个非常严酷的冰期环境 (Liu, 1985; Guo et al., 1998)，L₉ 中较高含量的 200~300 Ma 碎屑锆石可能反映了显著增强的来自西北的冬季风输送了更多的来自于中亚造山带的粗颗粒碎屑，并沉积于西宁盆地中，导致了晚古生代锆石含量的增加。

西宁黄土中前寒武纪碎屑锆石含量占 48%~52%，如此之高的含量在探讨物源过程中无法忽视。阿拉善干旱区、戈壁阿尔泰山南麓、祁连山北麓和柴达木盆地沉积物中均含有新元古代和古元古代锆石，但不同时期锆石的含量是有差别的。阿拉善干旱区和戈壁阿尔泰山南麓沉积物中具有约 1800 Ma 锆石年龄峰值 (图 6g)，柴达木盆地沉积物中 600~1000 Ma 锆石含量较高 (图 6d)，祁连山北麓沉积物中则 600~1000 Ma 和约 1800 Ma 锆石含量较高。祁连山北麓与柴达木盆地较高的 600~1000 Ma 锆石含量可能是祁连造山带中发育大规模与新元古代罗迪尼亞超大陆裂解相关的岩浆活动所导致的 (Song et al., 2013; 夏林圻等, 2016; Zuza et al., 2017)。祁连山北麓、柴达木盆地沉积物与西宁黄土新元古代碎屑锆石相对含量比阿拉善干旱区和戈壁阿尔泰山南麓沉积物的高，暗示了青藏高原北缘可能对西宁黄土中新元古代碎屑锆石的贡献更高。古元古代锆石的来源则较为复杂。大量的研究表明古元古代锆石广泛分布在阿拉善干旱区基岩中，如阿拉善地块的龙首山岩群 (修群业等, 2004; 耿元生等, 2006; Tung et al., 2007a) 与敦煌地块的 TTG 岩系 (Zhang et al., 2013; Zhao et al., 2015)，祁连地区的结晶基底、水系沉积物中 (Li, et al., 2007; Tung et al., 2017b; Zhang et al., 2020)，中亚造山带的基岩、沉积物中 (Che and Li, 2013; Wang et al., 2014; Xu et al., 2015; Zhang et al., 2016; 苏茂荣等, 2020)，不利于更好地识别西宁黄土古元古代锆石的主要物源。

3 结论

对西宁黄土不同层位黄土样品开展碎屑锆石 U-Pb 年代学研究，探讨其碎屑物质来源，并与黄土高原中—西部典型剖面进行差异对比，获得以下认识。

(1) 来自西宁黄土5个不同层位黄土样品的碎屑锆石具有多类型混合、磨圆度复杂、裂隙发育等特征, 表明锆石颗粒可能经历了强烈的物理风化以及多次再循环, 同时也可能暗示了西宁黄土为多物源混合。

(2) 5个样品的碎屑锆石U-Pb年龄谱分布特征较一致, 均具有早中生代—古生代(200~500 Ma)、新元古代(540~1000 Ma)、中元古代早期—古元古代中期(1400~2050 Ma)和古元古代早期—新太古代(2300~2800 Ma)的锆石年龄组, 表明西宁黄土物源在1.3 Ma以来没有显著变化。

(3) 西宁黄土与黄土高原典型黄土剖面的碎屑锆石年龄分布对比表明青藏高原东北缘的黄土堆积与黄土高原中—西部黄土的物源区应该是高度重合的, 但具有略微差异。

(4) 西宁黄土的碎屑锆石U-Pb年代学数据证明了青藏高原东北缘是中国黄土除中亚造山带之外另一处主要物源区, 同时也支持了中国黄土堆积是来自多个物源区的碎屑物质均匀混合的观点。

References

- AN Z S, 2000. The history and variability of the East Asian paleomonsoon climate [J]. Quaternary Science Reviews, 19 (1-5): 171-187.
- BIRD A, STEVENS T, RITTNER M, et al., 2015. Quaternary dust source variation across the Chinese Loess Plateau [J]. Palaeogeography, Palaeoclimatology, Palaeoecology, 435: 254-264.
- CHE X D, LI G J, 2013. Binary sources of loess on the Chinese Loess Plateau revealed by U-Pb ages of zircon [J]. Quaternary Research, 80 (3): 545-551.
- CHEN J, LI G J, YANG J D, et al., 2007. Nd and Sr isotopic characteristics of Chinese deserts: implications for the provenances of Asian dust [J]. Geochimica et Cosmochimica Acta, 71 (15): 3904-3914.
- CHEN J, LI G J, 2011. Geochemical studies on the source region of Asian dust [J]. Science China Earth Sciences, 54 (9): 1279-1301.
- CHEN Y, FANG X M, SONG C H, et al., 2012. The uplift and erosion of the Tianshan Mountains recorded by detrital zircon geochronology from the Cenozoic sediments in the southern Junggar Basin [J]. Earth Science Frontiers, 19 (5): 225-233. (in Chinese with English abstract)
- CHENG Y, LI X Q, ZHAO Z Y, et al., 2018. Detrital zircon U-Pb ages and its provenance significance in the TZK3 core from the Yangtze River delta [J]. Journal of Geomechanics, 24 (5): 635-644. (in Chinese with English abstract)
- CHU H, ZHANG J R, WEI C J, et al., 2013. A new interpretation of the tectonic setting and age of meta-basic volcanics in the Ondor Sum Group, Inner Mongolia [J]. Chinese Science Bulletin, 58 (28-29): 3580-3587.
- FENN K, STEVENS T, BIRD A, et al., 2018. Insights into the provenance of the Chinese Loess Plateau from joint zircon U-Pb and garnet geochemical analysis of last glacial loess [J]. Quaternary Research, 89 (3): 645-659.
- GEHRELS G E, YIN A, WANG X F, 2003. Detrital-zircon geochronology of the northeastern Tibetan plateau [J]. GSA Bulletin, 115 (7): 881-896.
- GENG Y S, WANG X S, SHEN Q H, et al., 2006. Redefinition of the Alxa Group-complex (Precambrian metamorphic basement) in the Alxa area, Inner Mongolia [J]. Geology in China, 33 (1): 138-145. (in Chinese with English abstract)
- GUO P, LIU C Y, WANG J Q, et al., 2017. Considerations on the application of detrital-zircon geochronology to sedimentary provenance analysis [J]. Acta Sedimentologica Sinica, 35 (1): 46-56. (in Chinese with English abstract)
- GUO Z T, LIU T, FEDOROFF N, et al., 1998. Climate extremes in Loess of China coupled with the strength of deep-water formation in the North Atlantic [J]. Global and Planetary Change, 18 (3-4): 113-128.
- HE X Y, FANG T H, BO H T, et al., 2022. Petrogenesis and tectonic significance of Late Permian-Middle Triassic granitoids in Guobaoshan, eastern section of the eastern Tianshan mountains: constraints from geochronology and geochemistry [J]. Journal of Geomechanics, 28 (1): 126-142.
- JAHN B M, GALLET S, HAN J M, 2001. Geochemistry of the Xining, Xifeng and Jixian sections, Loess Plateau of China: Eolian dust provenance and paleosol evolution during the last 140 ka [J]. Chemical Geology, 178 (1-4): 71-94.
- JI J F, CHEN J, LU H Y, 1999. Origin of illite in the loess from the Luochuan area, Loess Plateau, central China [J]. Clay Minerals, 34 (4): 525-532.
- JIAN P, LIU D Y, KRÖNER A, et al., 2008. Time scale of an early to mid-Paleozoic orogenic cycle of the long-lived Central Asian Orogenic Belt, Inner Mongolia of China: implications for continental growth [J]. Lithos, 101 (3-4): 233-259.
- LI G J, CHEN J, CHEN Y, et al., 2007. Dolomite as a tracer for the source regions of Asian dust [J]. Journal of Geophysical Research, 112 (D17): D17201.
- LI G J, CHEN J, JI J F, et al., 2009. Natural and anthropogenic sources of East Asian dust [J]. Geology, 37 (8): 727-730.
- LI G J, PETTKE T, CHEN J, 2011. Increasing Nd isotopic ratio of Asian dust indicates progressive uplift of the north Tibetan Plateau

- since the middle Miocene [J]. *Geology*, 39 (3): 199-202.
- LI G J, CHE X D, XIAO G Q, et al., 2013. Zircon ages of Xining loess: implication for the provenance of the loess on Chinese Loess Plateau [J]. *Quaternary Sciences*, 33 (2): 345-350. (in Chinese with English abstract)
- LI S Z, YANG Z, ZHAO S J, et al., 2016. Global Early Paleozoic Orogenes (II): subduction-accretionary-type orogeny [J]. *Journal of Jilin University (Earth Science Edition)*, 46 (4): 968-1004. (in Chinese with English abstract)
- LI Z, NIE S R, 1999. Xining loess deposition and its material sources, China [J]. *Earth Science-Journal of China University of Geosciences*, 24 (6): 581-584. (in Chinese with English abstract)
- LICHT A, PULLEN A, KAPP P, et al., 2016. Eolian cannibalism: reworked loess and fluvial sediment as the main sources of the Chinese Loess Plateau [J]. *GSA Bulletin*, 128 (5-6): 944-956.
- LIN X, LIU J, WU Z H, et al., 2021. Study on borehole provenance tracing and fluvial sediment diffusion in the Bohai Sea: double constraints from detrital zircon U-Pb age and in-situ geochemical element of apatite grains [J]. *Journal of Geomechanics*, 27 (2): 304-316. (in Chinese with English abstract)
- LIU D S, 1985. Loess and the environment [M]. Beijing: Science Press: 1-215. (in Chinese)
- LIU T, DING Z L, 1998. Chinese loess and the paleomonsoon [J]. *Annual Review of Earth and Planetary Sciences*, 26: 111-145.
- LU H Y, WANG X Y, WANG X Y, et al., 2012. Palaeoclimatic changes in northeastern Qinghai-Tibetan Plateau revealed by magnetostratigraphy and magnetic susceptibility analysis of thick loess deposits [J]. *Netherlands Journal of Geoscience-Geologie en Mijnbouw*, 91 (1-2): 187-198.
- MAHER B A, MUTCHE T J, CUNNINGHAM D, 2009. Magnetic and geochemical characteristics of Gobi Desert surface sediments: implications for provenance of the Chinese Loess Plateau [J]. *Geology*, 37 (3): 279-282.
- MAHER B A, PROSPERO J M, MACKIE D, et al., 2010. Global connections between Aeolian dust, climate and ocean biogeochemistry at the present day and at the last glacial maximum [J]. *Earth-Science Reviews*, 99 (1-2): 61-97.
- MAO L C, ZHANG F Q, FAN W M, et al., 2007. Phanerozoic evolution of the Inner Mongolia-Daxing'anling orogenic belt in North China: constraints from geochronology of ophiolites and associated formations [M] //ZHAIMG, WINDLEYBF, KUSKYTM, et al. Mesozoic sub-continental lithospheric thinning under eastern Asia. London: Geological Society of London, 280: 233-237.
- NIE J S, PENG W B, 2014. Automated SEM-EDS heavy mineral analysis reveals no provenance shift between glacial loess and interglacial paleosol on the Chinese Loess Plateau [J]. *Aeolian Research*, 13: 71-75.
- NIE J S, STEVENS T, RITTNER M, et al., 2015. Loess Plateau storage of Northeastern Tibetan Plateau-derived Yellow River sediment [J]. *Nature Communications*, 6: 8511.
- PULLEN A, KAPP P, MCCALLISTER A T, et al., 2011. Qaidam Basin and northern Tibetan Plateau as dust sources for the Chinese Loess Plateau and paleoclimatic implications [J]. *Geology*, 39 (11): 1031-1034.
- SONG S G, NIU Y L, SU L, et al., 2013. Tectonics of the North Qilian Orogen, NW China [J]. *Gondwana Research*, 23 (4): 1378-1401.
- SONG S G, NIU Y L, SU L, et al., 2014. Continental orogenesis from ocean subduction, continent collision/subduction, to orogen collapse, and orogen recycling: the example of the North Qaidam UHPM belt, NW China [J]. *Earth-Science Reviews*, 129: 59-84.
- STEVENS T, PALK C, CARTER A, et al., 2010. Assessing the provenance of loess and desert sediments in northern China using U-Pb dating and morphology of detrital zircons [J]. *GSA Bulletin*, 122 (7-8): 1331-1344.
- STEVENS T, CARTER A, WATSON T P, et al., 2013a. Genetic linkage between the Yellow River, the Mu Us desert and the Chinese Loess Plateau [J]. *Quaternary Science Reviews*, 78: 355-368.
- STEVENS T, ADAMIEC G, BIRD A F, et al., 2013b. An abrupt shift in dust source on the Chinese Loess Plateau revealed through high sampling resolution OSL dating [J]. *Quaternary Science Reviews*, 82: 121-132.
- SU M R, LI Y L, LIU H C, et al., 2020. Paleoproterozoic basement in eastern Central Asia Orogenic Belt: evidence from granite and sedimentary strata in Sino-Mongolia border area [J]. *Geology in China*, 47 (4): 1186-1203. (in Chinese with English abstract)
- SUN J M, DING Z L, XIA X P, et al., 2018. Detrital zircon evidence for the ternary sources of the Chinese Loess Plateau [J]. *Journal of Asian Earth Sciences*, 155: 21-34.
- SUN Y B, TADA R J, CHEN J C, et al., 2008. Tracing the provenance of fine-grained dust deposited on the central Chinese Loess Plateau [J]. *Geophysical Research Letters*, 35 (1): L01804.
- SUN Y B, YAN Y, NIE J S, et al., 2020. Source-to-sink fluctuations of Asian Aeolian deposits since the late Oligocene [J]. *Earth-Science Reviews*, 200: 102963.
- TUNG K A, YANG H Y, LIU D Y, et al., 2007a. SHRIMP U-Pb geochronology of the detrital zircons from the Longshoushan Group and its tectonic significance [J]. *Chinese Science Bulletin*, 52 (10): 1414-1425.
- TUNG K A, YANG H J, YANG H Y, et al., 2007b. SHRIMP U-Pb geochronology of the zircons from the Precambrian basement of the Qilian Block and its geological significances [J]. *Chinese Science Bulletin*, 52 (10): 2687-2701.
- VERMEESCH P, 2012. On the visualisation of detrital age distributions

- [J]. *Chemical Geology*, 312-313: 190-194.
- WANG X S, GAO J, KLEMD R, et al., 2014. Geochemistry and geochronology of the Precambrian high-grade metamorphic complex in the Southern Central Tianshan ophiolitic mélange, NW China [J]. *Precambrian Research*, 254: 129-148.
- WINDLEY B F, ALEXEIEV D, XIAO W J, et al., 2007. Tectonic models for accretion of the Central Asian Orogenic Belt [J]. *Journal of the Geological Society*, 164 (1): 31-47.
- WU C L, YANG J S, ROBINSON P T, et al., 2009. Geochemistry, age and tectonic significance of granitic rocks in north Altun, northwest China [J]. *Lithos*, 113 (3-4): 423-436.
- WU C L, CHEN H J, WU D, et al., 2018. Paleozoic granitic magmatism and tectonic evolution of the South Altun block, NW China: constraints from zircon U-Pb dating and Lu-Hf isotope geochemistry [J]. *Journal of Asian Earth Sciences*, 160: 168-199.
- XIA L Q, LI X M, YU J Y, et al., 2016. Mid-Late Neoproterozoic to Early Paleozoic volcanism and tectonic evolution of the Qilian Mountain [J]. *Geology in China*, 43 (4): 1087-1138. (in Chinese with English abstract)
- XIAO G Q, ZONG K Q, LI G J, et al., 2012. Spatial and glacial-interglacial variations in provenance of the Chinese Loess Plateau [J]. *Geophysical Research Letters*, 39 (20): L20715.
- XIAO W J, WINDLEY B F, HUANG B C, et al., 2009. End-Permian to mid-Triassic termination of the accretionary processes of the southern Altaids: implications for the geodynamic evolution, Phanerozoic continental growth, and metallogeny of Central Asia [J]. *International Journal of Earth Sciences*, 98 (6): 1189-1217.
- XIAO W J, WINDLEY B F, SUN S, et al., 2015. A tale of amalgamation of Three Permo-Triassic collage systems in central Asia: Oroclines, Sutures, and terminal accretion [J]. *Annual Review of Earth and Planetary Sciences*, 43: 477-507.
- XIE J, WU F Y, DING Z L, 2007. Detrital zircon composition of U-Pb ages and Hf isotope of the Hunshandake sandland and implications for its provenance [J]. *Acta Petrologica Sinica*, 23 (2): 523-528. (in Chinese with English abstract)
- XIE J, YANG S L, DING Z L, et al., 2012. Methods and application of using detrital zircons to trace the provenance of loess [J]. *Science ChinaEarth Sciences*, 55 (11): 1837-1846.
- XIU Q Y, YU H F, LI Q, et al., 2004. Discussion on the petrogenic time of Longshoushan Group, Gansu Province [J]. *Acta Geologica Sinica*, 78 (3): 366-373. (in Chinese with English abstract)
- XU X W, LI X H, JIANG N, et al., 2015. Basement nature and origin of the Junggar terrane: new zircon U-Pb-Hf isotope evidence from Paleozoic rocks and their enclaves [J]. *Gondwana Research*, 28 (1): 288-310.
- XU X Y, HE S P, WANG H L, et al., 2008. An Introduction to the geology of Northwest China: Qinling, Qilian and Tianshan regions [M]. Beijing: China Ocean Press.
- YANG H, ZHANG H F, LUO B J, et al., 2015. Early Paleozoic intrusive rocks from the eastern Qilian orogen, NE Tibetan Plateau: Petrogenesis and tectonic significance [J]. *Lithos*, 224-225: 13-31.
- YU S Y, ZHANG J X, LI S Z, et al., 2018. Continuity of the North Qilian and North Altun orogenic belts of NW China: evidence from newly discovered Palaeozoic Low-Mg and high-Mg adakitic rocks [J]. *Geological Magazine*, 155 (8): 1684-1704.
- YUAN Y, ZONG K Q, HE Z Y, et al., 2018. Geochemical evidence for Paleozoic crustal growth and tectonic conversion in the Northern Beishan Orogenic Belt, southern Central Asian Orogenic Belt [J]. *Lithos*, 302-303: 189-202.
- ZHANG H B, NIE J S, LIU X J, et al., 2021. Spatially variable provenance of the Chinese Loess Plateau [J]. *Geology*, 49 (10): 1155-1159.
- ZHANG H Z, LU H Y, XU X S, et al., 2016. Quantitative estimation of the contribution of dust sources to Chinese loess using detrital zircon U-Pb age patterns [J]. *Journal of Geophysical Research*, 121 (11): 2058-2099.
- ZHANG H Z, LU H Y, STEVENS T, et al., 2018. Expansion of dust provenance and aridification of Asia since ~ 7.2 Ma revealed by detrital zircon U-Pb dating [J]. *Geophysical Research Letters*, 45 (24): 13437-13448.
- ZHANG J X, YU S Y, GONG J H, et al., 2013. The latest Neoarchean-Paleoproterozoic evolution of the Dunhuang block, eastern Tarim craton, northwestern China: evidence from zircon U-Pb dating and Hf isotopic analyses [J]. *Precambrian Research*, 226: 21-42.
- ZHANG S, JIAN X, PULLEN A, et al., 2020. Tectono-magmatic events of the Qilian orogenic belt in northern Tibet: new insights from detrital zircon geochronology of river sands [J]. *International Geology Review*, 63 (8): 917-940.
- ZHANG S H, ZHAO Y, KRÖNER A, et al., 2009. Early Permian plutons from the northern North China Block: constraints on continental arc evolution and convergent margin magmatism related to the Central Asian Orogenic Belt [J]. *International Journal of Earth Sciences*, 98 (6): 1441-1467.
- ZHAO Y, SUN Y, YAN J H, et al., 2015. The Archean-Paleoproterozoic crustal evolution in the Dunhuang region, NW China: constraints from zircon U-Pb geochronology and in situ Hf isotopes [J]. *Precambrian Research*, 271: 83-97.
- ZHENG R G, WU T R, ZHANG W, et al., 2014. Late Paleozoic subduction system in the northern margin of the Alxa block, Altaids: geochronological and geochemical evidences from ophiolites [J]. *Gondwana Research*, 25 (2): 842-858.
- ZUZA A V, WU C, REITH R C, et al., 2017. Tectonic evolution of the Qilian Shan: an early Paleozoic orogen reactivated in the Cenozoic [J]. *GSA Bulletin*, 130 (5-6): 881-925.

附中文参考文献

- 陈熠, 方小敏, 宋春晖, 等, 2012. 准噶尔盆地南缘新生代沉积物碎屑锆石记录的天山隆升剥蚀过程 [J]. 地学前缘, 19 (5): 225-233.
- 程瑜, 李向前, 赵增玉, 等, 2018. 长江三角洲地区 TZK3 孔碎屑锆石 U-Pb 年龄及其物源意义 [J]. 地质力学学报, 24 (5): 635-644.
- 耿元生, 王新社, 沈其韩, 等, 2006. 内蒙古阿拉善地区前寒武纪变质基底阿拉善群的再厘定 [J]. 中国地质, 33 (1): 138-145.
- 郭佩, 刘池洋, 王建强, 等, 2017. 碎屑锆石年代学在沉积物源研究中的应用及存在问题 [J]. 沉积学报, 35 (1): 46-56.
- 贺昕宇, 方同辉, 薄贺天, 等, 2022. 东天山东段国宝山晚二叠世—中三叠世花岗质岩石成因与构造意义: 年代学和地球化学约束 [J]. 地质力学学报, 28 (1): 126-142.
- 李高军, 车旭东, 肖国桥, 等, 2013. 西宁黄土碎屑锆石年龄特征及其对黄土高原黄土物源的指示意义 [J]. 第四纪研究, 33 (2): 345-350.
- 李珍, 聂树人, 1999. 西宁黄土沉积及其物质来源 [J]. 地球科学: 中国地质大学学报, 24 (6): 581-584.
- 刘东生, 1985. 黄土与环境 [M]. 北京: 中国海洋出版社.
- 林旭, 刘静, 吴中海, 等, 2021. 渤海钻孔物源示踪和河流沉积物扩散研究: 碎屑锆石 U-Pb 年龄和磷灰石原位地球化学元素双重约束 [J]. 地质力学学报, 27 (2): 304-316.
- 苏茂荣, 李英雷, 刘汇川, 等, 2020. 中亚造山带东段古元古代结晶基底: 来自中蒙边境花岗岩和沉积地层的证据 [J]. 中国地质, 47 (4): 1186-1203.
- 夏林圻, 李向民, 余吉远, 等, 2016. 祁连山新元古代中—晚期至早古生代火山作用与构造演化 [J]. 中国地质, 43 (4): 1087-1138.
- 谢静, 吴福元, 丁仲礼, 2007. 浑善达克沙地的碎屑锆石 U-Pb 年龄和 Hf 同位素组成及其源区意义 [J]. 岩石学报, 23 (2): 523-528.
- 修群业, 于海峰, 李铨, 等, 2004. 龙首山岩群成岩时代探讨 [J]. 地质学报, 78 (3): 366-373.
- 徐学义, 何世平, 王洪亮, 等, 2008. 中国西北部地质概论: 秦岭、祁连、天山地区 [M]. 北京: 科学出版社.